
Regularizing Generative Models Using Knowledge of Feature Dependence

A PREPRINT

Naoya Takeishi, Yoshinobu Kawahara
RIKEN Center for Advanced Intelligence Project
naoya.takeishi@riken.jp

ABSTRACT

Generative modeling is a fundamental problem in machine learning with many potential applications. Efficient learning of generative models requires available prior knowledge to be exploited as much as possible. In this paper, we propose a method to exploit prior knowledge of relative dependence between features for learning generative models. Such knowledge is available, for example, when side-information on features is present. We incorporate the prior knowledge by forcing marginals of the learned generative model to follow a prescribed relative feature dependence. To this end, we formulate a regularization term using a kernel-based dependence criterion. The proposed method can be incorporated straightforwardly into many optimization-based learning schemes of generative models, including variational autoencoders and generative adversarial networks. We show the effectiveness of the proposed method in experiments with multiple types of datasets and models.

1 Introduction

Building models of natural and artificial phenomena is a fundamental problem in science and engineering. In statistical machine learning, generative modeling has been often intensively studied and discussed in terms of probabilistic graphical models (see, e.g., Koller & Friedman, 2009; Murphy, 2012). Recently, advances in deep neural network techniques have contributed to generative modeling as well; representative examples include variational autoencoders (VAEs) (Kingma & Welling, 2014) and generative adversarial networks (GANs) (Goodfellow et al., 2014).

Prior knowledge is indispensable for formulating feasible machine learning problems and solving them efficiently. In generative modeling, if one has detailed knowledge of the data-generating processes, they can be encoded into learning through carefully designing models and methods. For example, if one knows conditional independence between features, it can be encoded as a graphical model. Also, neural network architectures can be designed based on the knowledge of data properties; the success of convolutional neural networks would be largely due to its appropriateness to the nature of images. Generally speaking, however, it is usually too costly to prepare prior knowledge that can be directly utilized to design graphical models and neural network architectures. Moreover, the traditional knowledge-inducing techniques such as Bayesian inference with designed prior distributions are limited in their use cases.

It is also possible to exploit prior knowledge by regularization. On one hand, there are popular techniques used in diverse settings, such as Tikhonov regularization and sparsity regularization. Such regularization schemes reflect general knowledge of analysis and statistics that comply with a range of problems and datasets. On the other hand, methods to exploit prior knowledge specific to each dataset have been studied. For example, there are regularization schemes based on geometry of data manifolds (Belkin et al., 2006) and structured sparsity (Huang et al., 2011). Among many, the approach called posterior regularization (PR) (Ganchev et al., 2010) is widely used for imposing constraints on learned models. For instance, the PR in Bayesian inference (Zhu et al., 2014) was used for incorporating logical rules into topic models (Mei et al., 2014), and Hu et al. (2016b) used a

PR-like framework to reduce complexity of deep neural networks using logical rules. Moreover, Hu et al. (2018) proposed to combine PR and techniques of inverse reinforcement learning to automatically obtain a form of constraints from examples.

The purpose of this work lies in developing a framework to exploit prior knowledge of *feature dependence*, that is, how far a pair of variables is from statistical independence, for learning generative models. In applications of generative modeling, we often encounter this type of knowledge in at least a limited part of the data-generating process. For example, consider learning a generative model of sensor data for control or fault detection of a plant. In many practices, a system diagram of the plant is available, from which we may anticipate *relative* dependence between readings of *some* sensors attached to adjacent components. However, such incomplete signs of dependence can hardly be used to build a graphical model dedicated to the dataset. Hence, instead of designing a dedicated graphical model, such knowledge should be utilized in other ways.

Our idea is to utilize the knowledge of feature dependence for regularizing general-purpose generative models that have much flexibility. Let $p_\theta(\mathbf{x})$ be a generative model parameterized by a set of parameters θ . For incorporating the knowledge of feature dependence into $p_\theta(\mathbf{x})$, one straightforward way is to impose constraints on θ so that the statistical dependence between the marginals of $p_\theta(\mathbf{x})$ is consistent with this knowledge. However, we can hardly impose such complicated constraints explicitly. Therefore, in the proposed framework, we solve a relaxed problem that imposes regularization on the original learning problem.

The proposed method regularizes generative models so that they follow the prescribed knowledge of feature dependence. It is thus similar to PR but technically different to existing PR-like methods (Ganchev et al., 2010; Zhu et al., 2014; Hu et al., 2016b) as in our problem PR cannot be used directly. The regularization term in the proposed method is defined with a kernel-based dependence criterion of random variables (Gretton et al., 2005). It can be empirically computed and optimized if we can sample from the learned generative model $p_\theta(\mathbf{x})$ and if the gradient of a function of the samples is computable. These properties are shared by popular methods such as VAEs, GANs, and many others; the proposed regularizer is applicable to those methods and can be implemented without much additional work. Moreover, it is applicable to diverse types of data with appropriately designed kernels.

The remainder of this paper is organized as follows. In Section 2, we review generative modeling techniques and manifest the types of generative models to which the proposed method is applicable. In Section 3, we present the details of the proposed method. We introduce related work in Section 4 and experimental results in Section 5. This paper is concluded in Section 6.

2 Background: Learning Generative Models

Generative model is a term universally used in the machine learning community. In this paper, we use term “learning generative models” in a sense close to that of *density estimation*, in that we would like to learn $p_\theta(\mathbf{x})$, where \mathbf{x} denotes the observed random variable, and θ is the set of parameters to be estimated.

One popular type of generative modeling methodology utilizes probabilistic graphical models such as Bayesian networks and Markov random fields (see, e.g., Koller & Friedman, 2009; Murphy, 2012), which rely on probabilistic inference for learning. Moreover, methods based on deep neural networks (DNNs) have been intensively studied. Recent advances in this area include the development of VAEs (Kingma & Welling, 2014), GANs (Goodfellow et al., 2014), moment matching networks (Li et al., 2015), neural autoregressive models (e.g., Larochelle & Murray, 2011; van den Oord et al., 2016), and normalizing flows (e.g., Dinh et al., 2018; Kingma et al., 2016). As the number of parameters of a generative model increases, as is often the case with DNN-based methods, regularization based on prior knowledge becomes more crucial.

Many learning strategies for generative models are based on minimization of a loss function $L(\theta)$,

$$\underset{\theta}{\text{minimize}} L(\theta). \tag{1}$$

One standard type of loss function is a negative log-likelihood, i.e., $L(\theta) = -\log p_\theta(\mathbf{x})$. Many popular methods, such as EM-like algorithms for graphical models and estimation of normalizing flow models, follow (an approximated) likelihood-based learning. Another class of loss functions are those designed to perform comparison of model distribution and data distribution. This paradigm has been intensively studied recently for learning implicit generative models that have no explicit expression of likelihood. For example, GANs

(Goodfellow et al., 2014) are learned by minimizing Jensen–Shannon divergence between model distribution and data distribution via a two-player game.

The proposed regularization method presented in the next section is applicable to generative models with two properties, satisfied by many popular methods including VAEs and GANs (and their variants). They are informally described as follows:

Assumption 1 (Easy to sample). We can draw samples from $p_\theta(\mathbf{x})$ with an admissible computational cost.

Assumption 2 (Gradient of $\mathbb{E}_{p_\theta(\mathbf{x})}$). We can (approximately) compute $\nabla_{\theta} \mathbb{E}_{p_\theta(\mathbf{x})} [f(\mathbf{x})]$ for some function f of \mathbf{x} with an admissible computational cost.

3 Regularization Using Feature Dependence

First, let us clarify the terminology in this paper. We refer to each (set of) random variable in a multivariate dataset as a “feature” and use these terms interchangeably. Also, the term “dependence” is used in referring to statistical dependence, i.e., the gap from the statistical independence.

3.1 Motivation

In applications of generative modeling, knowledge of feature dependence is often available but not fully utilized. We particularly expect that we have knowledge of *relative* dependence between features of the data to be modeled. We illustrate this below using examples where such knowledge can and should be exploited.

One particular situation is when we have rough knowledge about the physical processes behind the data. For example, suppose we would like to model a dataset that comprises records from sensors in a plant (Figure 1a). We usually know which sensors are attached to which units in the plant and how those units are connected each other; we can expect sensor readings of the same or adjacent units to be relatively more dependent than those of non-connected units.

Another situation is when side-information of features is available. For example, suppose we would like to learn a generative model of a natural language corpus (Figure 1b). In this case, each feature corresponds to each word type in the corpus. Relative dependence between the words can be anticipated from word similarities obtained from external resources such as knowledge bases like WordNet (Miller, 1995) and word embeddings (see, e.g., Mikolov et al., 2013) learned using general large-scale corpora. Another example of useful side-information is geospatial information of sensors for sensor network data, where readings of sensors in proximity would be relatively dependent.

Note that, from such examples of knowledge of relative feature dependence alone, we can hardly prescribe precise conditional independence of each single feature. To this end, we would need deeper knowledge of underlying data-generating processes such as physical laws, and it would have to be described in a user-friendly way. This is why it is often impractical to manually build a full graphical model.¹ In our proposal, instead of manually designing graphical models, we aim to automatically regularize general-purpose generative models based on knowledge of feature dependence. One of the biggest advantages of this is that it can be applied to any parametric generative models as long as Assumptions 1 and 2 are satisfied.

Finally, let us consider an important question; does the knowledge of feature dependence really helps learning generative models? For some simple cases, the answer is easily understandable. For instance, consider the estimation of a multivariate normal distribution $\mathcal{N}_{\mathbf{x}}(\boldsymbol{\mu}, \boldsymbol{\Sigma})$ on $\mathbf{x} \in \mathbb{R}^d$. In this case, knowledge of feature dependence can be given as the difference of mutual information (MI) in the dimensions of \mathbf{x} , say $\text{MI}([\mathbf{x}]_i, [\mathbf{x}]_j) - \text{MI}([\mathbf{x}]_i, [\mathbf{x}]_k)$, which is proportional to

$$\log \left(\frac{\sqrt{[\boldsymbol{\Sigma}]_{ii}} - [\boldsymbol{\Sigma}]_{ij} / \sqrt{[\boldsymbol{\Sigma}]_{jj}}}{\sqrt{[\boldsymbol{\Sigma}]_{ii}} - [\boldsymbol{\Sigma}]_{ik} / \sqrt{[\boldsymbol{\Sigma}]_{kk}}} \right),$$

¹Learning structures of a graphical model from data (see, e.g., Murphy, 2012, Chapter 26) might be possible in some cases, but it is inherently difficult for general types and sizes of data.

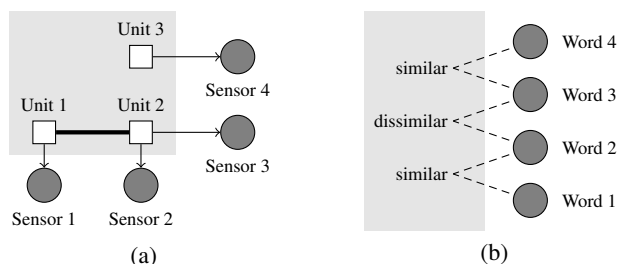


Figure 1: Examples of when knowledge of feature dependence is available. (a) When we know a part of the physical process; there would be stronger dependence between Sensor 1 and Sensors 2 & 3 than between Sensor 1 and Sensor 4, because Sensors 1, 2 & 3 are attached to the connected units. (b) When we have side-information such as word similarity provided by external resources; pairs of similar words would be more dependent than those of dissimilar words.

where $[\Sigma]_{ij}$ is the (i, j) -th element of Σ , for $i, j, k = 1, \dots, d$. If we can guess the sign² of this value *a priori*, we can impose a constraint on Σ , which would make the estimation somewhat easier in a statistical sense³ as the hypothesis space becomes smaller. Analyzing how learning is facilitated by knowledge in more general cases of complicated and misspecified models is an interesting open challenge.

3.2 Definition of Knowledge of Feature Dependence

Here we concretely define what we expect to serve as knowledge of feature dependence. We reiterate the point that the actual degree of feature dependence cannot be precisely described. Instead, what we select as prior knowledge is a guess of the dependence between a pair of features *relative to another pair*. This idea is written formally as follows.

Definition 1 (Knowledge of feature dependence). Suppose that the observed random variable, \mathbf{x} , is a tuple of d random variables, i.e., $\mathbf{x} = (x_1, \dots, x_d)$. Knowledge of feature dependence is described as a set of triples \mathcal{K} :

$$\mathcal{K} := \{(J_s^{\text{ref}}, J_s^+, J_s^-) \mid s = 1, \dots, |\mathcal{K}|\}, \quad (2)$$

where $J^{\text{ref}}, J^+, J^- \subset \{1, \dots, d\}$ are index sets. Its semantics are as follows: let $J = \{i_1, \dots, i_{|J|}\}$ and let \mathbf{x}_J be a subtuple of \mathbf{x} , i.e., $\mathbf{x}_J = (x_{i_1}, \dots, x_{i_{|J|}})$. The triple, $(J_s^{\text{ref}}, J_s^+, J_s^-)$, encodes the knowledge that $\mathbf{x}_{J_s^+}$ is more statistically dependent on $\mathbf{x}_{J_s^{\text{ref}}}$ than $\mathbf{x}_{J_s^-}$ is.

Example 1. We would choose $\mathcal{K} = \{(\{1\}, \{2, 3\}, \{4\})\}$ for the case of Figure 1a and $\mathcal{K} = \{(\{1\}, \{2\}, \{3, 4\})\}$ for the case of Figure 1b.

Example 2. Some other examples of \mathcal{K} are presented in Section 5 and the supplementary material.

3.3 Kernel-Based Dependence Criterion

There have been several types of methods proposed for measuring statistical dependence between random variables. Other than MI (see, e.g., Kraskov et al., 2004), well-known methods include mutual information correlation (Reshef et al., 2011) and distance correlation (Székely et al., 2007). In this work, we utilize a kernel-based dependence criterion, namely Hilbert–Schmidt independence criterion (HSIC) (Gretton et al., 2005). We use HSIC because it can be conveniently incorporated into objective functions of optimization problems as explained in the next subsection. In the remainder of this subsection, we introduce HSIC and related notions for completeness. Readers familiar with them may skip this subsection.

HSIC is defined and computed as follows (Gretton et al., 2005). Let p_{xy} be a joint measure over $(\mathcal{X} \times \mathcal{Y}, \Gamma \times \Lambda)$, where \mathcal{X} and \mathcal{Y} are separable spaces, Γ and Λ are Borel sets on \mathcal{X} and \mathcal{Y} , and (\mathcal{X}, Γ) and (\mathcal{Y}, Λ) are furnished

²We would not know the precise value of the relative MI as it depends on many factors.

³Complicated constraints makes the estimation difficult in a *computational* aspect. The proposed method avoids this difficulty and solves a relaxed regularized problem.

with probability measure p_x and p_y , respectively. Given separable reproducing kernel Hilbert spaces (RKHSs) \mathcal{F} and \mathcal{G} respectively on \mathcal{X} and \mathcal{Y} , HSIC is defined as the squared Hilbert–Schmidt norm of the associated cross-covariance operator C_{xy} , i.e., $\text{HSIC}(\mathcal{F}, \mathcal{G}, p_{xy}) := \|C_{xy}\|_{\text{HS}}^2$. When bounded kernels k and l are uniquely associated with the RKHSs, \mathcal{F} and \mathcal{G} , respectively, HSIC can be expressed in terms of expectations:

$$\begin{aligned} \text{HSIC}(\mathcal{F}, \mathcal{G}, p_{xy}) &= \mathbb{E}_{xx'yy'}[k(x, x', y, y')] + \mathbb{E}_{xx'}[k(x, x')]\mathbb{E}_{yy'}[k(y, y')] \\ &\quad - 2\mathbb{E}_{x,y}[\mathbb{E}_{x'}[k(x, x')]\mathbb{E}_{y'}[l(y, y')]]. \end{aligned} \quad (3)$$

One important fact is that $\text{HSIC} \geq 0$ and the equality holds if and only if x and y are statistically independent (Gretton et al., 2005, Theorem 4).

HSIC can be empirically estimated using a dataset $\mathcal{D} = \{(x_1, y_1), \dots, (x_m, y_m)\}$. Gretton et al. (2005) presented a biased estimator with $O(m^{-1})$ bias, and Song et al. (2012) proposed an unbiased estimator. In what follows, we denote an empirical estimation of $\text{HSIC}(\mathcal{F}, \mathcal{G}, p_{xy})$ computed from a dataset \mathcal{D} using HSIC by $\widehat{\text{HSIC}}_{x,y}(\mathcal{D})$. While the computation of empirical HSICs requires $O(m^2)$ operations, it may be sped up by methods such as random Fourier features (see, e.g., Zhang et al., 2018).

We now recall that what we would like to describe is the relative dependence of the features (Definition 1). Bounliphone et al. (2015) discussed the use of HSIC for a test of relative dependence. Let \mathcal{H} be a separable RKHS on a separable space \mathcal{Z} . Then, the test of relative dependence is formulated with the following null and alternative hypotheses:

$$\begin{aligned} H_0 &: \text{HSIC}(\mathcal{F}, \mathcal{G}, p_{xy}) \leq \text{HSIC}(\mathcal{F}, \mathcal{H}, p_{xz}), \quad \text{and} \\ H_1 &: \text{HSIC}(\mathcal{F}, \mathcal{G}, p_{xy}) > \text{HSIC}(\mathcal{F}, \mathcal{H}, p_{xz}). \end{aligned}$$

For this test, let

$$\hat{\rho}_{x,y,z} := \widehat{\text{HSIC}}_{x,y}(\mathcal{D}) - \widehat{\text{HSIC}}_{x,z}(\mathcal{D}). \quad (4)$$

From the asymptotic distribution of the unbiased empirical relative HSICs (Bounliphone et al., 2015), a conservative estimation of p -value of statistic $\hat{\rho}_{x,y,z}$ is given as

$$p \leq 1 - \Phi\left(\hat{\rho}_{x,y,z}(\sigma_{xy}^2 + \sigma_{xz}^2 - 2\sigma_{xyxz})^{-\frac{1}{2}}\right), \quad (5)$$

where Φ is the CDF of standard normal. See Bounliphone et al. (2015) for the definition of σ_{xy}^2 , σ_{xz}^2 , and σ_{xyxz} . Here, Eq. (5) means that under the null hypothesis, the probability that $\rho_{x,y,z}$ is greater than or equal to $\hat{\rho}_{x,y,z}$ is bounded. In the proposed method, we utilize this fact to formulate a regularization term.

3.4 Proposed Regularizer

We would like to force a generative model $p_\theta(\mathbf{x})$ to fulfill the prior knowledge encoded in the tuples in \mathcal{K} , the set defined in Eq. (2). For this purpose, the HSICs between the marginals of $p_\theta(\mathbf{x})$ must be consistent to \mathcal{K} ; that is, the HSIC between $p_\theta(\mathbf{x}_{J^{\text{ref}}})$ and $p_\theta(\mathbf{x}_{J^+})$ must be larger than that between $p_\theta(\mathbf{x}_{J^{\text{ref}}})$ and $p_\theta(\mathbf{x}_{J^-})$. More formally, as the result of optimization like Eq. (1), the marginals of $p_\theta(\mathbf{x})$ must satisfy constraints

$$\rho_s > 0, \quad \text{for } s = 1, \dots, |\mathcal{K}|, \quad (6)$$

$$\rho_s := \text{HSIC}(\mathcal{F}_{J_s^{\text{ref}}}, \mathcal{F}_{J_s^+}) - \text{HSIC}(\mathcal{F}_{J_s^{\text{ref}}}, \mathcal{F}_{J_s^-}), \quad (7)$$

where \mathcal{F}_J is a separable RKHS on the space of \mathbf{x}_J .

Since the population HSICs cannot be computed in general, directly imposing the constraints in Eq. (6) on the optimization, Eq. (1), is infeasible. Instead, we have the empirical estimation of the HSICs. With the empirical HSICs, it is possible for us to make $p_\theta(\mathbf{x})$ *probably* compatible with \mathcal{K} . In other words, we need to develop a method to make Eq. (6) probably satisfied. To this end, we constrain θ so that the null hypothesis (H_0 : “Eq. (6) is not satisfied”) is rejected in favor of the alternative hypothesis (H_1 : “Eq. (6) is satisfied”) with some statistical significance. We do this by imposing constraints on the bound of the p -value in Eq. (5) as

$$1 - \Phi\left(\hat{\rho}_s/\sigma_s\right) = \alpha, \quad \text{for } s = 1, \dots, |\mathcal{K}|, \quad (8)$$

Algorithm 1 Knowledge-regularized gradient method

Input: Dataset $\mathcal{D} = \{\mathbf{x}_i \in \mathbb{R}^d \mid i = 1, \dots, m\}$, knowledge set $\mathcal{K} = \{(J_s^{\text{ref}}, J_s^+, J_s^-) \mid s = 1, \dots, |\mathcal{K}|\}$, regularization parameter $\lambda > 0$, hyperparameter $\nu_\alpha > 0$

Output: A set of parameters θ^* of $p_\theta(\mathbf{x})$

- 1: initialize θ
- 2: **repeat**
- 3: compute $\frac{\partial L}{\partial \theta}$ $\triangleright L$ is the original objective
- 4: draw $\hat{\mathcal{D}} = \{\hat{\mathbf{x}}_i \in \mathbb{R}^d \mid i = 1, \dots, q\}$ from $p_\theta(\mathbf{x})$ \triangleright cf. Assumption 1
- 5: **for** $s = 1, \dots, |\mathcal{K}|$ **do**
- 6: $J_s \leftarrow J_s^{\text{ref}} \cup J_s^+ \cup J_s^-$
- 7: $\hat{\mathcal{D}}_s \leftarrow \{[\hat{\mathbf{x}}_i]_{J_s} \in \mathbb{R}^{|J_s|} \mid i = 1, \dots, q\}$ $\triangleright [\hat{\mathbf{x}}_i]_J$ is the subvector of $\hat{\mathbf{x}}_i$ indexed by J
- 8: compute $\frac{\partial \hat{\rho}_s}{\partial \theta}$ using $\hat{\mathcal{D}}_s$ \triangleright cf. Assumption 2
- 9: **end for**
- 10: compute $\frac{\partial R_{\mathcal{K}}}{\partial \theta}$ from $\{\frac{\partial \hat{\rho}_s}{\partial \theta} \mid s = 1, \dots, |\mathcal{K}|\}$
- 11: update θ using $\frac{\partial L}{\partial \theta} + \lambda \frac{\partial R_{\mathcal{K}}}{\partial \theta}$
- 12: **until** convergence

where $\sigma_s := (\sigma_{J_s^{\text{ref}}, J_s^+}^2 + \sigma_{J_s^{\text{ref}}, J_s^-}^2 - 2\sigma_{J_s^{\text{ref}}, J_s^+} \sigma_{J_s^{\text{ref}}, J_s^-})^{\frac{1}{2}}$, and

$$\hat{\rho}_s := \widehat{\text{HSIC}}_{x_{J_s^{\text{ref}}}, x_{J_s^+}}(\mathcal{D}) - \widehat{\text{HSIC}}_{x_{J_s^{\text{ref}}}, x_{J_s^-}}(\mathcal{D}). \quad (9)$$

Here, $0 < \alpha < 1$ is a tunable hyperparameter, and it is semantically similar to the significance level of (possibly multiple) testing; the smaller α is, the higher significance we require for the null hypothesis to be rejected in favor of the alternative. Eq. (8) is rewritten more straightforwardly as

$$\hat{\rho}_s = \nu_\alpha, \quad \text{for } s = 1, \dots, |\mathcal{K}|, \quad (10)$$

where $\nu_\alpha := \sigma_s \Phi^{-1}(1 - \alpha)$.

Now we have derived the constraints, Eq. (10), which should be satisfied by the empirical HSICs of the marginals of $p_\theta(\mathbf{x})$. However, imposing these constraints to the optimization problem in Eq. (1) is still impractical as $\hat{\rho}_s$ is a complicated composition of the elements of θ . Therefore, we propose to solve a relaxed problem as follows.

Definition 2 (Knowledge-based regularization). Let L be the original loss function used for learning a generative model by the optimization in Eq. (1). The corresponding optimization problem regularized according to the prior knowledge defined as Eq. (2) is

$$\underset{\theta}{\text{minimize}} \quad L(\theta) + \lambda R_{\mathcal{K}}(\theta), \quad (11)$$

where $\lambda \geq 0$ is a regularization parameter, and

$$R_{\mathcal{K}}(\theta) := \frac{1}{|\mathcal{K}|} \sum_{s=1}^{|\mathcal{K}|} \max(0, \nu_\alpha - \hat{\rho}_s). \quad (12)$$

Remark 1. We apply the hinge-like $\max(0, \cdot)$ operation for preventing $\hat{\rho}_s$ from being larger than ν_α . This is important because making $\hat{\rho}_s$ too large corresponds to requiring a too strict significance level α , which may interfere with optimizing the original loss, $L(\theta)$.

Remark 2. ν_α should be tuned as a hyperparameter. We can estimate the value of ν_α once the kernel and α are determined, but as α is originally a hyperparameter to be tuned, tuning ν_α directly does not increase the workload. In the experiments in Section 5, we found that using small values such as .01 and .05 was sufficient for Gaussian kernels.

Recall that we premised the property of the target generative model as in Assumption 2. From this assumption, the gradient of $\hat{\rho}_s$ can be computed since it is expressed as an expectation of the kernel functions on \mathbf{x} (Eq. (3)). Therefore, if solutions of the original optimization, Eq. (1), are obtained by a gradient-based method, the

regularized version, Eq. (11), can be solved using the same gradient-based method, and the implementation is straightforward. The situation is especially simplified if the dataset is a set of d -dimensional vectors, i.e., $\mathcal{D} = \{\mathbf{x}_i \in \mathbb{R}^d \mid i = 1, \dots, m\}$. In the optimization process, sample $\hat{\mathcal{D}} = \{\hat{\mathbf{x}}_i \in \mathbb{R}^d \mid i = 1, \dots, q\}$ from $p_\theta(\mathbf{x})$ being learned, and use them for estimating the empirical HSICs, the regularization term in Eq. (12), and their derivatives. Then, incorporate them into the original gradient-based updates. These procedures are summarized in Algorithm 1.

4 Related Work

4.1 Learning with Feature Similarity / Dependence

While knowledge of feature similarity or dependence has been previously utilized in machine learning in various contexts, none of these methods are directly applicable to our problem, i.e., regularizing generative models using knowledge of relative feature dependence.

Regarding supervised learning, meta-information of features such as pixel location in images was used for designing prior of weights of SVM (Krupka & Tishby, 2007) and for feature selection (Krupka et al., 2008). Regularization of linear models using feature similarity was considered by some researchers (Li & Li, 2008; Sandler et al., 2009; Li et al., 2017), and Mollaysa et al. (2017) considered the similarity-based regularization of nonlinear models. There is another line of studies on sparsity regularization whose patterns are designed following graphs on features (Huang et al., 2011). Moreover, prediction on graphs inherently utilizes feature similarity (see, e.g., Wu et al., 2019).

Such knowledge has also been utilized in unsupervised learning problems. For example, Tagawa et al. (2015) proposed a denoising autoencoder whose denoising structure is determined from prior knowledge of feature similarity, and Takeishi & Akimoto (2018) used similarity of features for designing prior of weights of linear generative models. In addition, there are studies on utilizing side-information for better solving problems such as robust PCA (Chiang et al., 2016) and collaborative filtering (Dong et al., 2017).

In the context of natural language processing, similarity of features (i.e., words) can often be obtained from knowledge on the semantic relations of words. For example, Xie et al. (2015) utilized correlations of words for topic modeling. Liu et al. (2015) utilized semantic similarity of words for learning word embeddings, and we note that the way they utilized the similarity is close to the proposed method.

Other than similarity of features, similarities of labels (Deng et al., 2014; Li et al., 2017; Wang et al., 2018) and similarities of objects (datapoints) (Belkin et al., 2006) have also been utilized in machine learning. Furthermore, we can regard multitask learning (see, e.g., Ando & Zhang, 2005) as a utilization of similarities between multiple tasks.

4.2 Learning with Constraints / Logical Rules

Facilitating machine learning using constraints or logical rules has also been intensively studied as a method to incorporate prior knowledge. For example, Mangasarian et al. (2004) proposed SVMs with constraints, and Schiegg et al. (2012) proposed the logic-based priors using Markov logic networks (Richardson & Domingos, 2006) for mixtures of Gaussian process regressors. In unsupervised learning, there is a line of studies on topic models with logical rules (Andrzejewski et al., 2011; Mei et al., 2014; Foulds et al., 2015). In this line, other researchers used taxonomy information (Yao et al., 2015; Hu et al., 2016a) and knowledge graph embeddings (Yao et al., 2017) for improving topics.

PR (posterior regularization) (Ganchev et al., 2010) is a powerful tool for integrating prior knowledge into machine learning models. Hu et al. (2016b) proposed a method that combines knowledge distillation (Hinton et al., 2015) and PR for incorporating fuzzy knowledge into DNNs. Also, a framework termed RegBayes (Zhu et al., 2014) was used for formulating topic models with logic rules (Mei et al., 2014). Moreover, Hu et al. (2018) pointed out the connection between PR and reinforcement learning and proposed a framework for learning constraints from examples.

Semantic-based regularization (Diligenti et al., 2012, 2017) is another principle for injecting logical rules into learning procedures. Diligenti et al. (2012) formulated functional-type constraints on functions being learned.

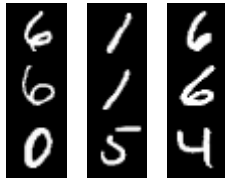


Figure 2: Three samples from the CCMNIST dataset we created. Each image comprises three digits concatenated in rows. The top and bottom ones are chosen from the images with the same label.

The constraints were designed based on fuzzy first-order logical rules and the theory of T-norms, with which logical clauses can be converted into real-valued functions.

4.3 Learning by Dependence Criteria

In our study we used a dependence criterion to build the proposed regularizer. Such dependence criteria have been previously used for similar purposes. For instance, Lopez et al. (2018) proposed to regularize VAEs using HSIC to make some latent variables independent so that the learned VAEs are compatible with prior knowledge of the data-generating process. This idea is similar to our proposed framework, with an important difference being that while Lopez et al. (2018) considered the regularization of encoders, we investigated the regularization of decoders. Also, while Lopez et al. (2018) considered independence of variables, our method is based on relative dependence.

In fairness-aware machine learning, dependence criteria are used to make outputs independent of sensitive variables. For example, Kamishima et al. (2012) proposed a regularization scheme using MI for logistic regression, and Pérez-Suay et al. (2017) used HSIC for regularizing regression models. In the method called variational fair autoencoder (Louizos et al., 2016), the latent variable is forced to be independent of the values of sensitive variables.

Using dependence criteria for learning itself is also an active area of study. For example, Hjelm et al. (2018) proposed learning deep generative models by maximizing MI between input data and the encoder’s output. Moreover, Belghazi et al. (2018) proposed a trick to estimate MI using neural networks and used it for learning GANs.

5 Experiments

We examined the effects of the proposed regularization using multiple types of datasets and generative models. The details of the experiments not described below are presented in the supplementary material.

5.1 Datasets and Prior Knowledge

5.1.1 Toy Data

We prepared a cylinder-shaped toy dataset generated by

$$\mathbf{x} = [\cos(2\pi z_1) \quad \sin(2\pi z_1) \quad 2z_2]^\top + \mathbf{e}, \quad (13)$$

where $z_1, z_2 \sim \text{uniform}(0, 1)$ and $\mathbf{e} \sim \mathcal{N}(\mathbf{0}, 10^{-4} \mathbf{I})$.

On this dataset, we know that x_1 and x_2 are more statistically dependent than x_1 and x_3 are. This prior knowledge is expressed in the manner of Eq. (2) as

$$\mathcal{K}_{\text{Toy}} = \{(J_1^{\text{ref}} = \{1\}, J_1^+ = \{2\}, J_1^- = \{3\})\}. \quad (14)$$

5.1.2 Concatenated MNIST

We created a dataset from the MNIST handwritten digit images, namely concatenated MNIST (termed CCMNIST hereafter). Some examples are shown in Figure 2. Each image in this dataset is generated by vertically

concatenating three MNIST images. Here, the concatenation is constrained so that the top image and the middle image have the same label, whereas there is no constraint on the label of the bottom image; it is chosen independently from the top two. We created training and validation sets from MNIST’s training dataset and a test set from MNIST’s test dataset.

On this dataset, we can anticipate that the top third and the middle third of images are more statistically dependent than the top and the bottom are. If each image is vectorized in a row-wise fashion, this knowledge is expressed as

$$\mathcal{K}_{\text{ccMNIST}} = \{(J_1^{\text{ref}} = \{1, \dots, 28^2\}, J_1^+ = \{28^2 + 1, \dots, 28^2 \times 2\}, J_1^- = \{28^2 \times 2 + 1, \dots, 28^2 \times 3\})\}. \quad (15)$$

5.1.3 Plant Sensor Data

We used a simulated sensor dataset, which we term PLANT hereafter. The simulation is based on a real industrial chemical plant called Tennessee Eastman process (Downs & Vogel, 1993). In the plant, there are four major unit operations: reactor, vapor-liquid separator, recycle compressor, and product stripper. On each unit operation, sensors such as level sensors and thermometers are attached. We used readings of 22 sensors. We divided the original datasets of normal operation into training, validation, and test sets. Note that the dataset is multivariate time-series but we treated it as a set of independent observations of dimensionality 22.

On this dataset, we can anticipate relative dependence between sets of sensors based on the process diagram of the plant (Downs & Vogel, 1993). For example, the knowledge set for this dataset, $\mathcal{K}_{\text{Plant}}$, contains

$$(J^{\text{ref}} = J_{\text{compressor}}, J^+ = J_{\text{reactor}}, J^- = J_{\text{stripper}}), \quad (16)$$

where $J_{\text{compressor}}$ denote the set of indices of sensors regarding the recycle compressor, and J_{reactor} and J_{stripper} are analogously defined. This is plausible because the reactor is directly connected to the recycle compressor but the product stripper is not. See the supplementary material for the detailed definition of $\mathcal{K}_{\text{Plant}}$ and J ’s.

5.1.4 Solar Energy Production Data

We used the records of solar power production⁴, which we term SOLAR hereafter. We extracted a dataset comprising recordings of power production of 137 solar power plants in Alabama in June 2006. The data of the first 20 days were used for training, the next five days were for validation, and the last five days were for testing. This dataset was also treated as a set of independent observations.

On this dataset, we can anticipate dependence of features from geometric distances between the solar plants. We created a knowledge set $\mathcal{K}_{\text{Solar}}$ as follows; for the i -th plant ($i = 1, \dots, 137$), if the nearest plant is within 10 [km] and the distance to the second-nearest plant is more than 12 [km], then add $(\{i\}, \{j_i\}, \{k_i\})$ to $\mathcal{K}_{\text{Solar}}$, where j_i and k_i are the indices of the nearest and the second-nearest plants, respectively. This resulted in $\mathcal{K}_{\text{Solar}}$ with 31 tuples.

5.2 General Settings

We learned factor analysis (FA) models, VAEs, and GANs using the datasets introduced in Section 5.1. See the supplementary material for the details of the generative models. They were learned with or without the proposed regularizer based on the prior knowledge. Regardless of whether the proposed regularizer was used or not, weight decay was adopted in every learning process.

For the proposed method, we computed the empirical HSICs using the sample of size $|\hat{\mathcal{D}}| = 128$ and Gaussian kernels with the bandwidth chosen according to the median heuristics. The hyperparameters, λ and ν_α , were chosen according to the performance on the validation sets. Note that the hyperparameter search was not intensive; λ was chosen from only three candidate values that roughly adjust orders of L and $R_{\mathcal{K}}$, and ν_α was chosen from .01 or .05.

Table 1: A part of test reconstruction errors by FA models. Averages (standard deviations) over 10 random trials are shown.

	w/o regularization	with regularization
CCMNIST	1.84 (0.001)	1.69 (0.001)
PLANT	$3.32 (0.05) \times 10^4$	$3.30 (0.03) \times 10^4$
SOLAR	$3.19 (0.03) \times 10^4$	$3.11 (0.03) \times 10^4$

Table 2: A part of test negative ELBOs of VAEs. Averages (standard deviations) over 10 random trials are shown.

	w/o regularization	with regularization
TOY	65.5 (20)	60.9 (25)
CCMNIST	$3.71 (0.02) \times 10^2$	$3.63 (0.01) \times 10^2$
PLANT	$9.15 (0.33) \times 10^4$	<i>$8.84 (0.32) \times 10^4$</i>
SOLAR	$4.77 (1.6) \times 10^5$	$1.76 (0.29) \times 10^5$

bold: $p < 10^{-3}$ *italic:* $p < 10^{-2}$

5.3 Results and Discussion

5.3.1 Evaluation by Test Set Performance

We learned FAs and VAEs on the TOY⁵, CCMNIST, PLANT, and SOLAR datasets. For VAEs, the encoder and the decoder were modeled with multi-layer perceptrons with three fully-connected hidden layers. These models can be evaluated by examining the values of the respective loss functions on test sets: reconstruction errors for FAs and (negative) evidence lower bounds (ELBOs) for VAEs. We conducted experiments with 10 different random seeds. A part of the results is shown in Tables 1 and 2, and the experimental results not shown here are presented in the supplementary material. According to the p -values calculated based on t -tests, the proposed regularization method resulted in significant improvement in many cases.

For comparison, we designed a VAE decoder dedicated to the CCMNIST dataset in accordance with the prior knowledge that the top and the middle parts of the images are digits of the same type (see the supplementary for details). VAEs with the dedicated decoder scored $3.51 (0.04) \times 10^2$ by average test ELBOs, which is basically better than the performance by the proposed method (3.63×10^2 ; see Table 2). In other words, the proposed regularizer performed intermediately between the most general model (no regularization, no special decoder) and the tailored model with the carefully designed decoder.

5.3.2 Learning Curves

For understanding the effects of the regularization in more detail, we examined learning curves of VAEs on the CCMNIST dataset, which are shown in Figure 3. We can observe that while the training losses decrease to the same extent, the test loss remains smaller when the knowledge-based regularization is applied. It is also observed that when the regularization is applied, the test loss intermittently increases and decreases rapidly. This is probably because the regularizer, $R_{\mathcal{K}}$, takes non-zero values intermittently due to the $\max(0, \cdot)$ operation and changes the direction of optimizer’s updates in those occasions. This phenomenon is not a crucial drawback, but developing a method for preventing this may facilitate more stable learning.

5.3.3 Effect of Knowledge Set Size

Another interest lies in how the amount of provided prior knowledge affects the performance of the proposed regularizer. We investigated this by changing the number of tuples in $\mathcal{K}_{\text{Solar}}$ in learning VAEs using the SOLAR dataset. As the original knowledge set, $\mathcal{K}_{\text{Solar}}$, comprises 31 tuples, we created four knowledge subsets by

⁴www.nrel.gov/grid/solar-power-data.html

⁵We did not tried FA on the TOY data because it is meaningless.

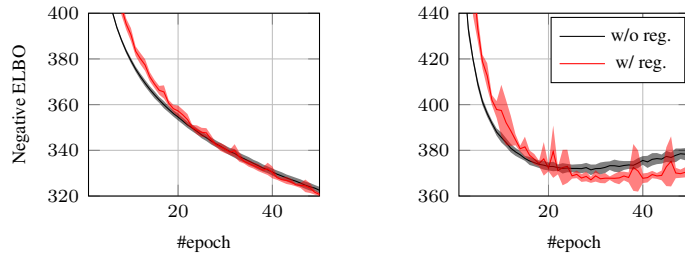


Figure 3: Learning curves of VAEs on the CCMNIST dataset: (*left*) for the training set and (*right*) for the test set. Averages and standard deviations over 10 random trials are shown.

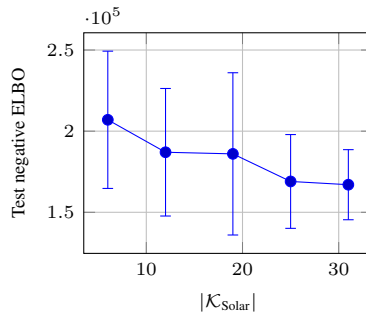


Figure 4: Performance of VAEs learned on the SOLAR dataset with regularization given by $\mathcal{K}_{\text{Solar}}$ of different sizes from 6 to 31. The averages and the standard deviations over 10 random trials are shown.

extracting 6, 12, 19, and 25 tuples from the original set, respectively. When creating the subsets, tuples were chosen so that a larger subset contains all elements of a smaller subset. In Figure 4, the test set performances of VAEs regularized with $\mathcal{K}_{\text{Solar}}$ of different sizes are shown. We can observe that the performance is improved with larger $\mathcal{K}_{\text{Solar}}$'s. The difference between the test ELBO of $|\mathcal{K}| = 6$ and that of $|\mathcal{K}| = 31$ is significant with $p = .003$ by a t -test.

5.3.4 Inspection of Generated Samples

We learned GANs using the TOY dataset and inspected the samples drawn from the learned models. We often observed that, when the regularizer was not applied, a phenomenon similar to “mode collapse” (see, e.g., Metz et al., 2017) occurred as in the left-side plots of Figure 5. On the other hand, the whole geometry of the TOY data was basically learned successfully with the proposed regularizer (the right panel of Figure 5). We did not expect this effect beforehand, but this implies its effectiveness on learning GANs, which should be elaborated in the future.

6 Conclusion

In this work, we have developed a regularization scheme for generative models that allows the marginals of the learned model to be compatible with prescribed knowledge of relative feature dependence. The proposed regularizer can be easily incorporated into generative models such as graphical models, VAEs, GANs, and many others.

In future studies, direct improvements to the proposed framework should be possible. For example, higher-order dependence between multiple sets of features can be considered using an extension of HSIC (Pfister et al., 2017). A possible drawback of the current proposed method is the difficulty of selecting appropriate kernels. Hence, the use of more tuning-free dependence criteria such as mutual information neural estimation (Belghazi et al., 2018) is worth investigating. Effective use of prior knowledge is one of the big challenges in machine learning, as issues such as the treatment of uncertainty in prior knowledge remain to be solved.

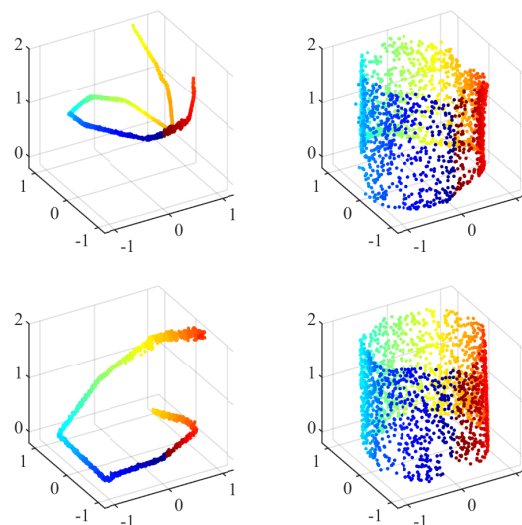


Figure 5: Samples from GANs learned on the TOY dataset: (*left*) without the regularization and (*right*) with the regularization. The top and the bottom rows are with different random seeds.

Acknowledgments

This work was supported by JSPS KAKENHI Grant No. JP18H06487.

References

- Ando, R. K. and Zhang, T. A framework for learning predictive structures from multiple tasks and unlabeled data. *Journal of Machine Learning Research*, 6:1817–1853, 2005.
- Andrzejewski, D., Zhu, X., Craven, M., and Recht, B. A framework for incorporating general domain knowledge into latent Dirichlet allocation using first-order logic. In *Proceedings of the 22nd International Joint Conference on Artificial Intelligence*, pp. 1171–1177, 2011.
- Belghazi, M. I., Baratin, A., Rajeswar, S., Ozair, S., Bengio, Y., Courville, A., and Hjelm, R. D. Mutual information neural estimation. arXiv:1801.04062, 2018.
- Belkin, M., Niyogi, P., and Sindhvani, V. Manifold regularization: A geometric framework for learning from labeled and unlabeled examples. *Journal of Machine Learning Research*, 7:2399–2434, 2006.
- Bounliphone, W., Gretton, A., Tenenhaus, A., and Blaschko, M. B. A low variance consistent test of relative dependency. In *Proceedings of the 32nd International Conference on Machine Learning*, pp. 20–29, 2015.
- Chiang, K.-Y., Hsieh, C.-J., and Dhillon, I. Robust principal component analysis with side information. In *Proceedings of The 33rd International Conference on Machine Learning*, pp. 2291–2299, 2016.
- Deng, J., Ding, N., Jia, Y., Frome, A., Murphy, K., Bengio, S., Li, Y., Neven, H., and Adam, H. Large-scale object classification using label relation graphs. In *Lecture Notes in Computer Science*, volume 8689, pp. 48–64, 2014.
- Diligenti, M., Gori, M., Maggini, M., and Rigutini, L. Bridging logic and kernel machines. *Machine Learning*, 86(1):57–88, 2012.
- Diligenti, M., Gori, M., and Saccá, C. Semantic-based regularization for learning and inference. *Artificial Intelligence*, 244:143–165, 2017.
- Dinh, L., Sohl-Dickstein, J., and Bengio, S. Density estimation using real NVP. In *Proceedings of the 6th International Conference on Learning Representations*, 2018.

- Dong, X., Yu, L., Wu, Z., Sun, Y., Yuan, L., and Zhang, F. A hybrid collaborative filtering model with deep structure for recommender systems. In *Proceedings of the 31st AAAI Conference on Artificial Intelligence*, pp. 1309–1315, 2017.
- Downs, J. J. and Vogel, E. F. A plant-wide industrial process control problem. *Computers & Chemical Engineering*, 17(3):245–255, 1993.
- Foulds, J., Kumar, S. H., and Getoor, L. Latent topic networks: A versatile probabilistic programming framework for topic models. In *Proceedings of the 32nd International Conference on Machine Learning*, pp. 777–786, 2015.
- Ganchev, K., Graça, J., Gillenwater, J., and Taskar, B. Posterior regularization for structured latent variable models. *Journal of Machine Learning Research*, 11:2001–2049, 2010.
- Goodfellow, I., Pouget-Abadie, J., Mirza, M., Xu, B., Warde-Farley, D., Ozair, S., Courville, A., and Bengio, Y. Generative adversarial nets. In *Advances in Neural Information Processing Systems 27*, pp. 2672–2680, 2014.
- Gretton, A., Bousquet, O., Smola, A., and Schölkopf, B. Measuring statistical dependence with Hilbert–Schmidt norms. In *Algorithmic Learning Theory*, pp. 63–77, 2005.
- Hinton, G., Vinyals, O., and Dean, J. Distilling the knowledge in a neural network. arXiv:1503.02531, 2015.
- Hjelm, R. D., Fedorov, A., Lavoie-Marchildon, S., Grewal, K., Bachman, P., Trischler, A., and Bengio, Y. Learning deep representations by mutual information estimation and maximization. arXiv:1808.06670, 2018.
- Hu, Z., Luo, G., Sachan, M., Xing, E., and Nie, Z. Grounding topic models with knowledge bases. In *Proceedings of the 25th International Joint Conference on Artificial Intelligence*, pp. 1578–1584, 2016a.
- Hu, Z., Ma, X., Liu, Z., Hovy, E., and Xing, E. P. Harnessing deep neural networks with logic rules. In *Proceedings of the 54th Annual Meeting of the Association for Computational Linguistics*, pp. 2410–2420, 2016b.
- Hu, Z., Yang, Z., Salakhutdinov, R., Liang, X., Qin, L., Dong, H., and Xing, E. P. Deep generative models with learnable knowledge constraints. In *Advances in Neural Information Processing Systems 31*, 2018.
- Huang, J., Zhang, T., and Matas, D. Learning with structured sparsity. *Journal of Machine Learning Research*, 12:3371–3412, 2011.
- Kamishima, T., Akaho, S., Asoh, H., and Sakuma, J. Fairness-aware classifier with prejudice remover regularizer. In *Lecture Notes in Computer Science*, volume 7524, pp. 35–50, 2012.
- Kingma, D. P. and Ba, J. L. Adam: A method for stochastic optimization. In *Proceedings of the 3rd International Conference on Learning Representations*, 2015.
- Kingma, D. P. and Welling, M. Auto-encoding variational Bayes. In *Proceedings of the 2nd International Conference on Learning Representations*, 2014.
- Kingma, D. P., Salimans, T., Jozefowicz, R., Chen, X., Sutskever, I., and Welling, M. Improved variational inference with inverse autoregressive flow. In *Advances in Neural Information Processing Systems 29*, pp. 4743–4751, 2016.
- Koller, D. and Friedman, N. *Probabilistic Graphical Models: Principles and Techniques*. The MIT Press, 2009.
- Kraskov, A., Stögbauer, H., and Grassberger, P. Estimating mutual information. *Physical Review E*, 69:066138, 2004.
- Krupka, E. and Tishby, N. Incorporating prior knowledge on features into learning. In *Proceedings of the 11th International Conference on Artificial Intelligence and Statistics*, pp. 227–234, 2007.
- Krupka, E., Navot, A., and Tishby, N. Learning to select features using their properties. *Journal of Machine Learning Research*, 9:2349–2376, 2008.
- Larochelle, H. and Murray, I. The neural autoregressive distribution estimator. In *Proceedings of the 14th International Conference on Artificial Intelligence and Statistics*, pp. 29–37, 2011.
- Li, C. and Li, H. Network-constrained regularization and variable selection for analysis of genomic data. *Bioinformatics*, 24(9):1175–1182, 2008.
- Li, Y., Swersky, K., and Zemel, R. Generative moment matching networks. In *Proceedings of the 32nd International Conference on International Conference on Machine Learning*, pp. 1718–1727, 2015.

- Li, Y., Yang, M., Xu, Z., and Zhang, Z. M. Learning with feature network and label network simultaneously. In *Proceedings of the 31st AAAI Conference on Artificial Intelligence*, pp. 1410–1416, 2017.
- Liu, Q., Jiang, H., Wei, S., Ling, Z.-H., and Hu, Y. Learning semantic word embeddings based on ordinal knowledge constraints. In *Proceedings of the 53rd Annual Meeting of the Association for Computational Linguistics and the 7th International Joint Conference on Natural Language Processing*, pp. 1501–1511, 2015.
- Lopez, R., Regier, J., Jordan, M. I., and Yosef, N. Information constraints on auto-encoding variational Bayes. In *Advances in Neural Information Processing Systems 31*, 2018.
- Louizos, C., Swersky, K., Li, Y., Welling, M., and Zemel, R. The variational fair autoencoder. In *Proceedings of the 4th International Conference on Learning Representations*, 2016.
- Mangasarian, O. L., Shavlik, J. W., and Wild, E. W. Knowledge-based kernel approximation. *Journal of Machine Learning Research*, 5:1127–1141, 2004.
- Mei, S., Zhu, J., and Zhu, X. Robust RegBayes: Selectively incorporating first-order logic domain knowledge into Bayesian models. In *Proceedings of the 31st International Conference on Machine Learning*, pp. 253–261, 2014.
- Metz, L., Poole, B., Pfau, D., and Sohl-Dickstein, J. Unrolled generative adversarial networks. In *Proceedings of the 5th International Conference on Learning Representations*, 2017.
- Mikolov, T., Sutskever, I., Chen, K., Corrado, G. S., and Dean, J. Distributed representations of words and phrases and their compositionality. In *Advances in Neural Information Processing Systems 26*, pp. 3111–3119, 2013.
- Miller, G. A. WordNet: A lexical database for English. *Communications of the ACM*, 38(11):39–41, 1995.
- Mollaysa, A., Strasser, P., and Kalousis, A. Regularising non-linear models using feature side-information. In *Proceedings of the 34th International Conference on Machine Learning*, pp. 2508–2517, 2017.
- Murphy, K. P. *Machine Learning: A Probabilistic Perspective*. The MIT Press, 2012.
- Pérez-Suay, A., Laparra, V., Mateo-García, G., Muñoz-Marí, J., Gómez-Chova, L., and Camps-Valls, G. Fair kernel learning. In *Lecture Notes in Computer Science*, volume 10534, pp. 339–355, 2017.
- Pfister, N., Bühlmann, P., Schölkopf, B., and Peters, J. Kernel-based tests for joint independence. *Journal of the Royal Statistical Society: Series B*, 80(1):5–31, 2017.
- Reshef, D. N., Reshef, Y. A., Finucane, H. K., Grossman, S. R., McVean, G., Turnbaugh, P. J., Lander, E. S., Mitzenmacher, M., and Sabeti, P. C. Detecting novel associations in large data sets. *Science*, 334(6062): 1518–1524, 2011.
- Richardson, M. and Domingos, P. Markov logic networks. *Machine Learning*, 62(1-2):107–136, 2006.
- Sandler, T., Blitzer, J., Talukdar, P. P., and Ungar, L. H. Regularized learning with networks of features. In *Advances in Neural Information Processing Systems 21*, pp. 1401–1408, 2009.
- Schiegg, M., Neumann, M., and Kersting, K. Markov logic mixtures of Gaussian processes: Towards machines reading regression data. In *Proceedings of the 15th International Conference on Artificial Intelligence and Statistics*, pp. 1002–1011, 2012.
- Song, L., Smola, A., Gretton, A., Bedo, J., and Borgwardt, K. Feature selection via dependence maximization. *Journal of Machine Learning Research*, 13:1393–1434, 2012.
- Székely, G. J., Rizzo, M. L., and Bakirov, N. K. Measuring and testing dependence by correlation of distances. *The Annals of Statistics*, 35(6):2769–2794, 2007.
- Tagawa, T., Tadokoro, Y., and Yairi, T. Structured denoising autoencoder for fault detection and analysis. In *Proceedings of the 6th Asian Conference on Machine Learning*, pp. 96–111, 2015.
- Takeishi, N. and Akimoto, K. Knowledge-based distant regularization in learning probabilistic models. arXiv:1806.11332, 2018.
- van den Oord, A., Kalchbrenner, N., and Kavukcuoglu, K. Pixel recurrent neural networks. In *Proceedings of the 33rd International Conference on Machine Learning*, pp. 1747–1756, 2016.

- Wang, G., Li, C., Wang, W., Zhang, Y., Shen, D., Zhang, X., Henao, R., and Carin, L. Joint embedding of words and labels for text classification. In *Proceedings of the 56th Annual Meeting of the Association for Computational Linguistics*, pp. 2321–2331, 2018.
- Wu, Z., Pan, S., Chen, F., Long, G., Zhang, C., and Yu, P. S. A comprehensive survey on graph neural networks. arXiv:1901.00596, 2019.
- Xie, P., Yang, D., and Xing, E. Incorporating word correlation knowledge into topic modeling. In *Proceedings of the 2015 Conference of the North American Chapter of the Association for Computational Linguistics: Human Language Technologies*, pp. 725–734, 2015.
- Yao, L., Zhang, Y., Wei, B., Qian, H., and Wang, Y. Incorporating probabilistic knowledge into topic models. In *Advances in Knowledge Discovery and Data Mining*, volume 9078 of *Lecture Notes in Computer Science*, pp. 586–597, 2015.
- Yao, L., Zhang, Y., Wei, B., Jin, Z., Zhang, R., Zhang, Y., and Chen, Q. Incorporating knowledge graph embeddings into topic modeling. In *Proceedings of the 31st AAAI Conference on Artificial Intelligence*, pp. 3119–3126, 2017.
- Zhang, Q., Filippi, S., Gretton, A., and Sejdinovic, D. Large-scale kernel methods for independence testing. *Statistics and Computing*, 28(1):113–130, 2018.
- Zhu, J., Chen, N., and Xing, E. P. Bayesian inference with posterior regularization and applications to infinite latent SVMs. *Journal of Machine Learning Research*, 15:1799–1847, 2014.

A Detailed Settings of Experiments

A.1 Datasets and Knowledge Sets

A.1.1 Toy Data

In creating the TOY data, we generated 1,000 samples for a training set, 2,000 samples for a validation set, and another 2,000 samples for a test set.

A.1.2 Concatenated MNIST

In creating the CCMNIST data, we generated a training set of size 20,000 and a validation set of size 10,000 from MNIST’s training dataset and a test set of size 10,000 from MNIST’s test dataset.

A.1.3 Plant Sensor Data

Dataset We used the Tennessee Eastman (TE) process data available online⁶, which were generated using `teprob.f`⁷ originally provided by the authors of Downs & Vogel (1993). We downloaded `d00.dat` and `d00_te.dat`, which contained the data generated with the normal operating condition, and created three sets from them. We used the whole `d00.dat` for a training set (size 500) and divided `d00_te.dat` into a validation set (size 400) and a test set (size 560). The original data consist of 12 manipulated variables and 41 process measurement variables. Within the process measurement variables, we used the measurements of the level sensors, flow rate sensors, thermometers, and manometers, which finally composed the 22-dimensional data. As preprocessing, we normalized the data using the values of average and standard deviation of each variable of the training set. Moreover, we added noise following $\mathcal{N}(0, 10^{-4})$.

Knowledge set Based on the sensor locations shown in the process diagram of the TE process (Downs & Vogel, 1993), we classified each of the 22 variables into one of the following seven groups: Feed 1, Feed 2, Reactor, Vapor-liquid separator, Recycle compressor, Product stripper, and Purge. This grouping is built upon

⁶github.com/camaramm/tennessee-eastman-profBraatz [retrieved 30 December 2018].

⁷The code and the related materials are also archived online at depts.washington.edu/control/LARRY/TE/download.html.

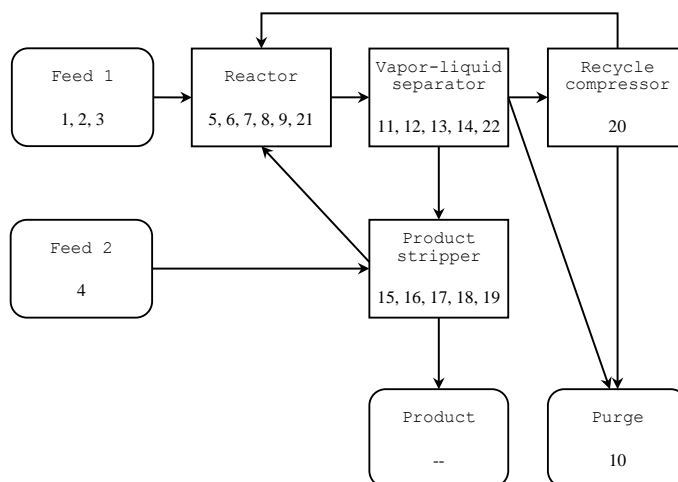


Figure 6: Diagram of the units in the TE process drawn by the authors referring to the original one (Downs & Vogel, 1993). The numbers below the unit names are the sensor indices corresponding to each unit. The grouping of the sensors is by the authors of this manuscript and not necessarily complete nor general.

the unit structure of the TE process. The units are interconnected in the process as shown in Figure 6, according to which we designed the knowledge set, $\mathcal{K}_{\text{plant}}$, as follows:

$$\mathcal{K}_{\text{Solar}} = \left\{ (J_{\text{Reactor}}, J_{\text{Separator}}, J_{\text{Feed2}}), (J_{\text{Reactor}}, J_{\text{Separator}}, J_{\text{Purge}}), (J_{\text{Separator}}, J_{\text{Stripper}}, J_{\text{Feed1}}), \right. \\ (J_{\text{Separator}}, J_{\text{Stripper}}, J_{\text{Feed2}}), (J_{\text{Separator}}, J_{\text{Compressor}}, J_{\text{Feed1}}), (J_{\text{Separator}}, J_{\text{Compressor}}, J_{\text{Feed2}}), \\ (J_{\text{Compressor}}, J_{\text{Reactor}}, J_{\text{Feed1}}), (J_{\text{Compressor}}, J_{\text{Reactor}}, J_{\text{Feed2}}), (J_{\text{Compressor}}, J_{\text{Reactor}}, J_{\text{Stripper}}), \\ \left. (J_{\text{Stripper}}, J_{\text{Reactor}}, J_{\text{Feed1}}), (J_{\text{Stripper}}, J_{\text{Reactor}}, J_{\text{Purge}}), (J_{\text{Stripper}}, J_{\text{Reactor}}, J_{\text{Compressor}}) \right\},$$

where

$$J_{\text{Feed1}} = \{1, 2, 3\}, \quad J_{\text{Feed2}} = \{4\}, \quad J_{\text{Reactor}} = \{5, 6, 7, 8, 9, 21\}, \quad J_{\text{Separator}} = \{11, 12, 13, 14, 22\}, \\ J_{\text{Stripper}} = \{15, 16, 17, 18, 19\}, \quad J_{\text{Compressor}} = \{20\}, \quad \text{and} \quad J_{\text{Purge}} = \{10\}.$$

A.1.4 Solar

Dataset The SOLAR dataset was created from the data provided at the website of National Renewable Energy Laboratory⁸. We downloaded the set of csv files (a1-pv-2006.zip) containing power production records of solar plants in Alabama state and concatenated the contents of the 137 files as the 137-dimensional dataset. We used the data of June 2006 because the seasonal variation seemed moderate in that period. We subsampled the original data (sampled every five minutes) by 1/3 and divided them into a training set (days 1–20), a validation set (days 21–25), and a test set (days 26–30). Finally the size of each set is 1,920, 480, and 480, respectively. Because the data contain many zero values, we added 10^{-3} to the whole datasets and took natural logarithm, which resulted in the data valued approximately from -6 to 4 . As preprocessing, we normalized the data using the values of average and standard deviation of each variable of the training set. Moreover, we added noise following $\mathcal{N}(0, 10^{-4})$.

Knowledge set Knowledge set was created following scheme presented in the main manuscript.

A.2 Generative Models

A.2.1 Factor Analysis Model

In the factor analysis (FA) model we used, the observed variable, $\mathbf{x} \in \mathbb{R}^d$, is modeled as

$$\mathbf{x} \approx \mathbf{W}\mathbf{z} + \boldsymbol{\mu}, \quad (17)$$

⁸www.nrel.gov/grid/solar-power-data.html [retrieved 9 January 2019].

Table 3: Sets of candidates for hyperparameter λ , from which λ was chosen by validation performance.

Model	Dataset	Candidates for λ
FA	CCMNIST	$5 \times 10^3, 10^4$, or 2×10^4
	PLANT	$2.5 \times 10^4, 5 \times 10^4$, or 10^5
	SOLAR	$5 \times 10^4, 10^5$, or 2×10^5
VAE	TOY	250, 500, or 1000
	CCMNIST	$5 \times 10^3, 10^4$, or 2×10^4
	PLANT	$2.5 \times 10^4, 5 \times 10^4$, or 10^5
	SOLAR	$2.5 \times 10^5, 5 \times 10^5$, or 10^6

Table 4: Settings of dimensionality of \mathbf{z} and MLP’s hidden layers used in the experiments.

Model	Dataset	dim(\mathbf{z})	dim(MLP-hidden)
FA	CCMNIST	200, 800	—
	PLANT	7, 11	—
	SOLAR	13, 54	—
VAE	TOY	4	32
	CCMNIST	50, 100, 200	512, 1024, 2048
	PLANT	4, 7, 11	32, 64, 128
	SOLAR	4, 13, 54	128, 256, 512
GAN	TOY	4	32

where $\mathbf{z} \in \mathbb{R}^p$ ($p \leq d$) is a latent variable, which is inferred by

$$\tilde{\mathbf{z}} = \mathbf{W}^\top(\mathbf{x} - \boldsymbol{\mu}). \quad (18)$$

The parameters, \mathbf{W} and $\boldsymbol{\mu}$, are learned by minimizing the following square loss:

$$\|\mathbf{x} - \mathbf{W}\mathbf{W}^\top(\mathbf{x} - \boldsymbol{\mu}) - \boldsymbol{\mu}\|_2^2. \quad (19)$$

This model can be regarded as a linear autoencoder with the constrained encoder and decoder. The detailed settings are described in Section A.3.

A.2.2 Variational Autoencoder

A variational autoencoder (VAE) (Kingma & Welling, 2014) is learned via maximization of the evidence lower bound (ELBO):

$$\text{ELBO} = \mathbb{E}_{q_{\theta_{\text{enc}}}(\mathbf{z}|\mathbf{x})}[\log p_{\theta_{\text{dec}}}(\mathbf{x}|\mathbf{z})] - \text{KL}(q_{\theta_{\text{enc}}}(\mathbf{z}|\mathbf{x}) \parallel p_{\theta_{\text{dec}}}(\mathbf{x}|\mathbf{z})), \quad (20)$$

where $p_{\theta_{\text{dec}}}(\mathbf{x}|\mathbf{z})$ and $q_{\theta_{\text{enc}}}(\mathbf{z}|\mathbf{x})$ are a decoder and an encoder having sets of parameters, θ_{dec} and θ_{enc} , respectively. We modeled the encoder and the decoder using multi-layer perceptrons (MLPs) in every experiment. The detailed settings are described in Section A.3.

A.2.3 Generative Adversarial Network

A generative adversarial network (GAN) (Goodfellow et al., 2014) is learned via minimization of the following cross-entropy loss:

$$\log D_{\theta_D}(\mathbf{x}) + \log(1 - D_{\theta_D}(G_{\theta_G}(\mathbf{z}))), \quad (21)$$

where G_{θ_G} and D_{θ_D} are a generator and a discriminator with having sets of parameters, θ_G and θ_D , respectively. In GANs, the generator generates fake samples while the discriminator tries to distinguish the fake and the real data. We modeled the generator and the discriminator using MLPs. The detailed settings are described in Section A.3.

A.3 Experiment Settings

For settings that are not described below, we used the default values of PyTorch 0.4.1.

A.3.1 Hyperparameter Tuning

The hyperparameters of the proposed method were chosen in accordance with the validation set performance. The set of candidates for ν_α was just $\{.01, .05\}$ for every experiment. The sets of candidates for λ are shown in Table 3. The candidate values of λ were set so that the orders of the original loss function and the regularizer were roughly adjusted.

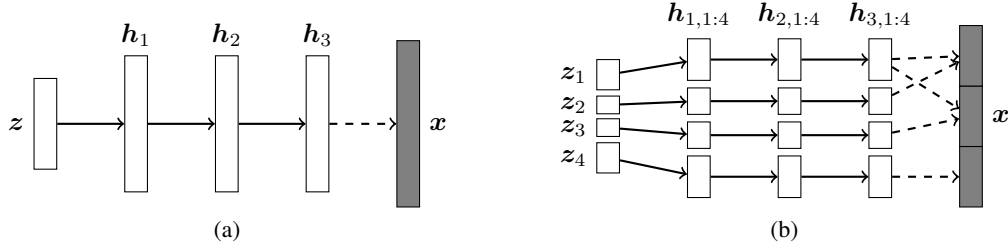


Figure 7: Architectures of (a) the decoder modeled by a general fully-connected MLP and (b) the decoder specially designed for CCMNIST dataset. In both diagrams, z is the latent variable of VAE, h 's are the hidden layers of the decoder, and x denotes the observed variable. The solid arrows represent affine transformation followed by the ReLU function, and the dashed arrows represent affine transformation.

A.3.2 Architectures

The encoder / decoder of VAEs and the generator / discriminator of GANs were modeled using MLPs. Each MLP has fully-connected three hidden layers, each of which has the same number of units. The dimensionality of z and the number of units of MLP's hidden layers are summarized in Table 4. The dimensionality of z was determined basically in accordance with the cumulative contributing rates (i.e., explained variance) of PCA on the PLANT and SOLAR datasets. As for the PLANT dataset, 4 principal components (PCs) explain 99% variance, 7 PCs explain 99.9%, and 11 PCs explain 99.99%; analogously for the SOLAR dataset.

For the MLPs, we used ReLU as the activation function except for the VAE on the SOLAR dataset. For the VAE on the SOLAR dataset, we used tanh.

In the experiment of VAE on the CCMNIST dataset, for a reference of performance, we also tried a dedicated decoder architecture. In the tailored decoder, the latent variable, z , was divided into four parts as $z = [z_1^T z_2^T z_3^T z_4^T]^T$. Then, the top third of each image is modeled only with z_1 and z_2 , the middle third is with z_1 and z_3 , and the bottom third is with z_4 . The detail of the tailored decoder is shown in Figure 7b. This tailored structure reflects the fact that the top and the middle parts of the images are from the same digit while the bottom is independent from the top two.

A.3.3 Optimization

Every optimization was done using Adam optimizer (Kingma & Ba, 2015). α , one of the parameters of Adam, was basically 0.001 with a few exception; we used $\alpha = 0.0005$ for learning the FA model on the PLANT dataset and for the GAN on the TOY dataset. Also, we used $\beta_1 = 0.5$ for GANs and $\beta_1 = 0.9$ otherwise.

B Detailed Experimental Results

In Tables 5 and 6, we present the full results of the experiment introduced in Section 5.3.1 of the main manuscript.

Table 5: Test reconstruction errors by FA models. Averages (standard deviations) over 10 random trials are shown. The results in **red** rows are also shown in the main manuscript.

Dataset	dim(z)	w/o regularization	with regularization
ccMNIST	200	1.07 (0.004)	1.06 (0.016) ***
	800	1.84 (0.001)	1.69 (0.001) ***
PLANT	7	$5.41 (0.04) \times 10^4$	$5.42 (0.03) \times 10^4$
	11	$3.32 (0.05) \times 10^4$	$3.30 (0.03) \times 10^4$
SOLAR	13	$6.83 (0.07) \times 10^4$	$6.78 (0.05) \times 10^4$ *
	54	$3.19 (0.03) \times 10^4$	$3.11 (0.03) \times 10^4$ ***

Table 6: Test negative ELBOs of VAEs. Averages (standard deviations) over 10 random trials are shown. The results in **red** rows are also shown in the main manuscript.

Dataset	dim(z)	dim(MLP-hidden)	w/o regularization	with regularization	with tailored decoder
TOY	4	32	65.5 (20)	60.9 (25)	—
ccMNIST	50	512	$3.75 (0.03) \times 10^2$	$3.65 (0.01) \times 10^2$ ***	$3.66 (0.03) \times 10^2$
	50	1024	$3.67 (0.02) \times 10^2$	$3.60 (0.02) \times 10^2$ ***	$3.49 (0.03) \times 10^2$
	50	2048	$3.67 (0.03) \times 10^2$	$3.63 (0.03) \times 10^2$ **	$3.43 (0.01) \times 10^2$
	100	512	$3.75 (0.01) \times 10^2$	$3.67 (0.02) \times 10^2$ ***	$3.66 (0.03) \times 10^2$
	100	1024	$3.71 (0.02) \times 10^2$	$3.63 (0.01) \times 10^2$ ***	$3.51 (0.04) \times 10^2$
	100	2048	$3.68 (0.02) \times 10^2$	$3.65 (0.02) \times 10^2$ *	$3.43 (0.01) \times 10^2$
	200	512	$3.78 (0.02) \times 10^2$	$3.71 (0.01) \times 10^2$ ***	$3.67 (0.04) \times 10^2$
	200	1024	$3.72 (0.03) \times 10^2$	$3.66 (0.02) \times 10^2$ ***	$3.51 (0.03) \times 10^2$
200	2048	$3.70 (0.01) \times 10^2$	$3.68 (0.03) \times 10^2$	$3.44 (0.01) \times 10^2$	
PLANT	4	32	$1.04 (0.04) \times 10^5$	$1.01 (0.03) \times 10^5$ *	—
	4	64	$1.03 (0.04) \times 10^5$	$1.02 (0.02) \times 10^5$	—
	4	128	$1.04 (0.04) \times 10^5$	$1.02 (0.02) \times 10^5$ *	—
	7	32	$9.88 (0.53) \times 10^4$	$9.39 (0.37) \times 10^4$ ***	—
	7	64	$9.15 (0.33) \times 10^4$	$8.84 (0.32) \times 10^4$	—
	7	128	$9.13 (0.16) \times 10^4$	$9.02 (0.32) \times 10^4$	—
	11	32	$9.73 (0.62) \times 10^4$	$9.50 (0.65) \times 10^4$	—
	11	64	$8.92 (0.52) \times 10^4$	$8.57 (0.36) \times 10^4$ **	—
11	128	$7.99 (0.32) \times 10^4$	$7.77 (0.38) \times 10^4$ **	—	
SOLAR	4	128	$9.53 (4.6) \times 10^5$	$3.03 (0.85) \times 10^5$ ***	—
	4	256	$7.85 (1.5) \times 10^5$	$3.46 (0.99) \times 10^5$ ***	—
	4	512	$6.35 (1.2) \times 10^5$	$3.47 (0.83) \times 10^5$ ***	—
	13	128	$5.41 (6.1) \times 10^5$	$2.06 (0.31) \times 10^5$	—
	13	256	$4.77 (1.6) \times 10^5$	$1.76 (0.29) \times 10^5$ ***	—
	13	512	$5.21 (0.94) \times 10^5$	$2.26 (0.50) \times 10^5$ ***	—
	54	128	$3.49 (6.0) \times 10^5$	$1.68 (0.13) \times 10^5$	—
	54	256	$3.44 (1.0) \times 10^5$	$1.65 (0.28) \times 10^5$ ***	—
54	512	$8.99 (0.87) \times 10^5$	$4.19 (0.83) \times 10^5$ ***	—	

Significant difference between “w/o regularization” and “with regularization” with
 ***: $p < 10^{-3}$, **: $p < 10^{-2}$, or *: $p < 5 \times 10^{-2}$.